560 **Supplements**

Landsat 8 imagery

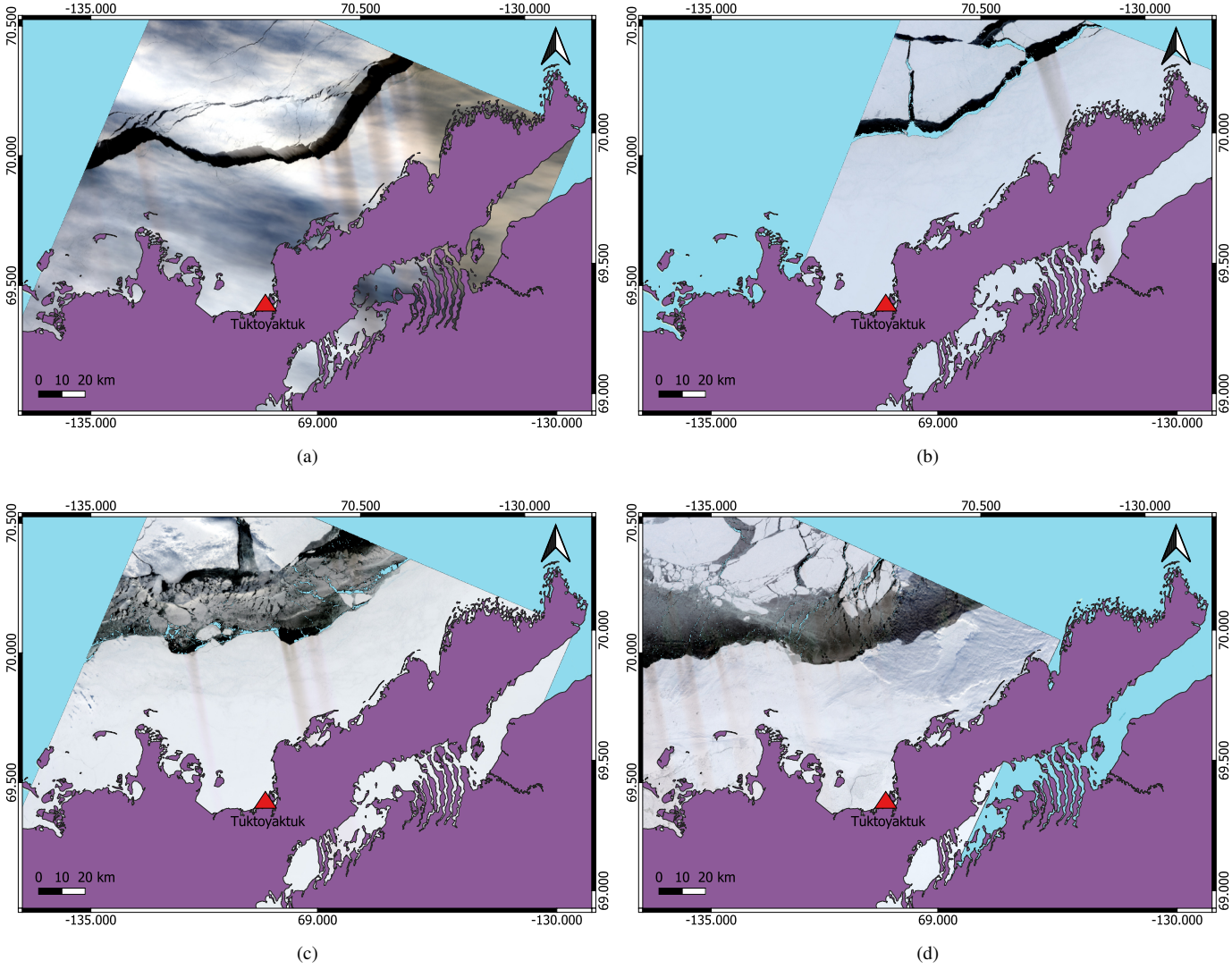
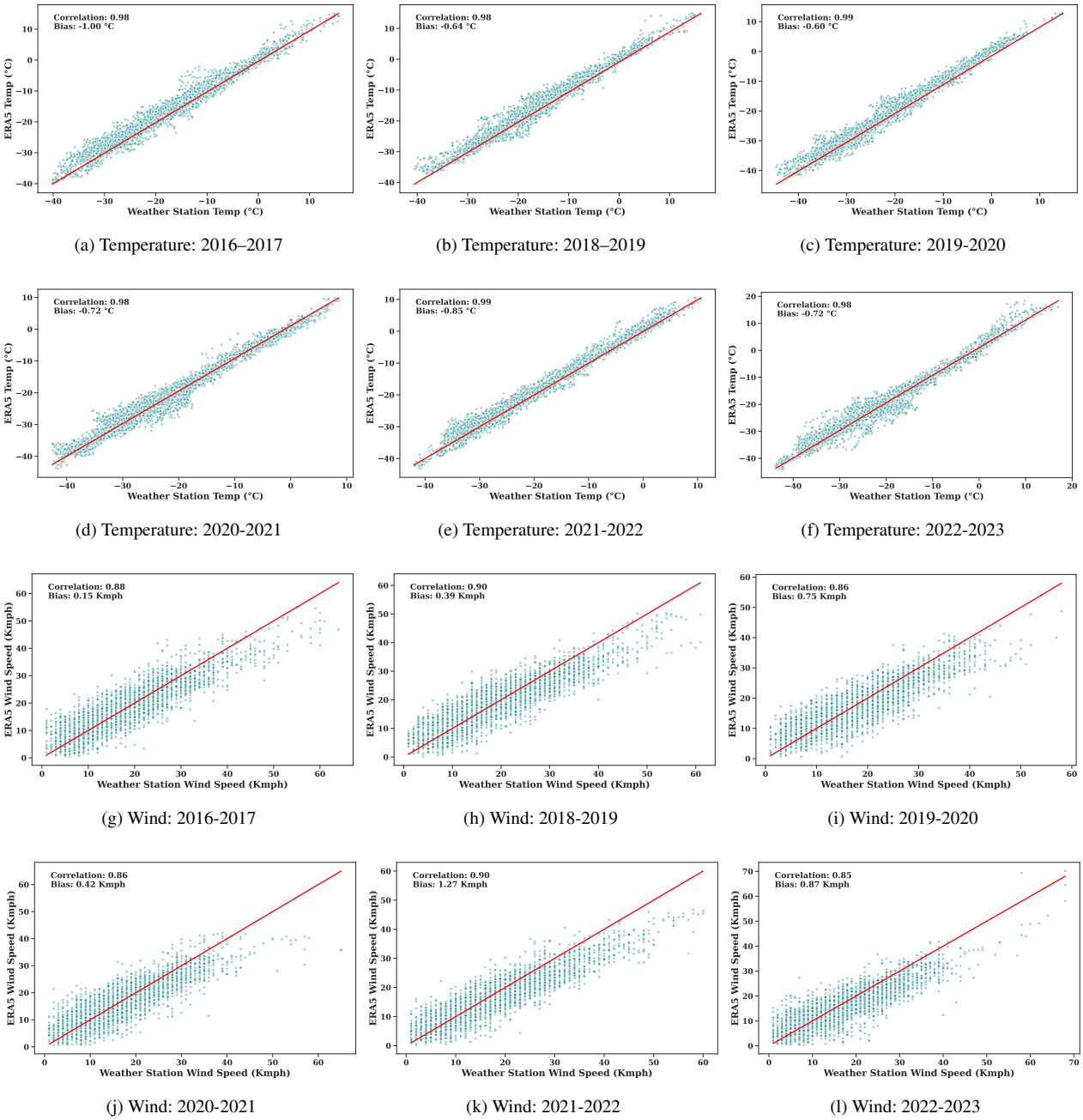


Figure S1. Landsat 8 imagery for dates (a) 2020-03-07, (b) 2020-04-01, (c) 2020-04-08, (d) 2022-03-04 showing examples of fracture openings and flaw lead development between LFSI and adjacent pack ice.



(a) Temperature: 2016–2017 (b) Temperature: 2018–2019 (c) Temperature: 2019-2020

(d) Temperature: 2020-2021 (e) Temperature: 2021-2022 (f) Temperature: 2022-2023

(g) Wind: 2016-2017 (h) Wind: 2018-2019 (i) Wind: 2019-2020

(j) Wind: 2020-2021 (k) Wind: 2021-2022 (l) Wind: 2022-2023

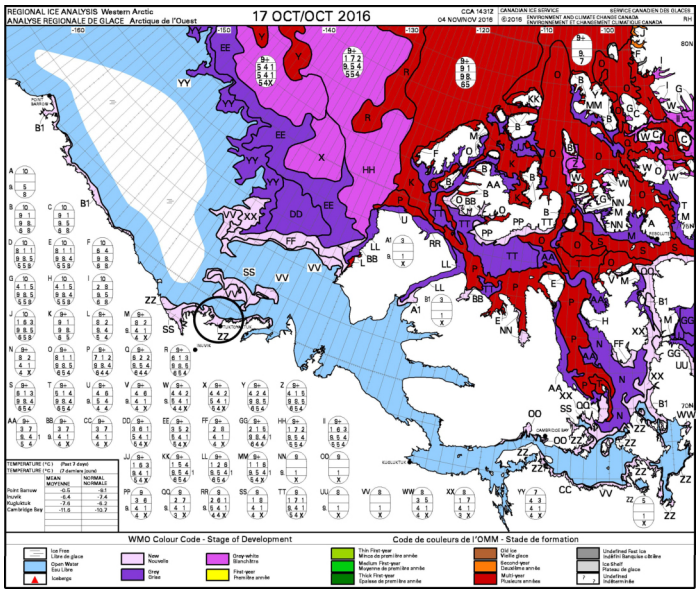
Figure S2. Plots showing the degree of agreement between ERA5 and weather station data at 69.430°N, 133.03°W for Temperature in top two rows from (a) 2016-2017 to (f) 2022-2023 and Wind Speed in bottom two rows from (g) 2016-2017 to (l) 2022-2023.

ERA5 vs weather station

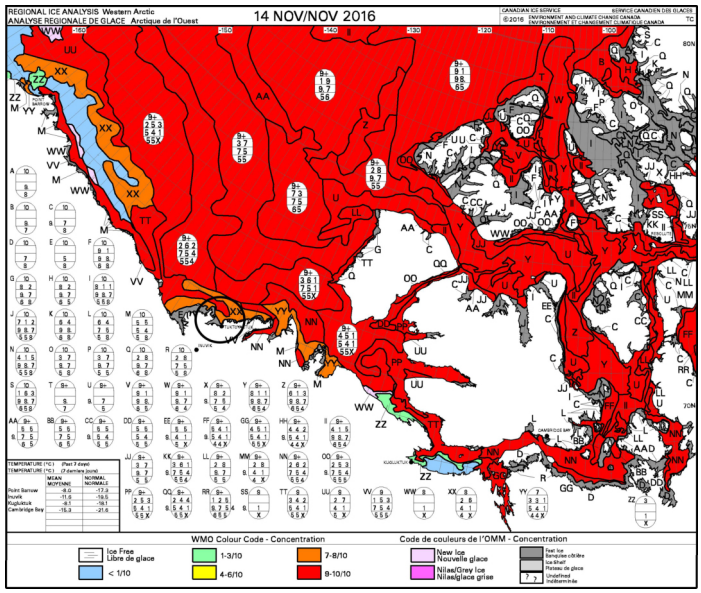
Sea Ice Charts

2016-2017

New Ice



Fast Ice



Ice Free

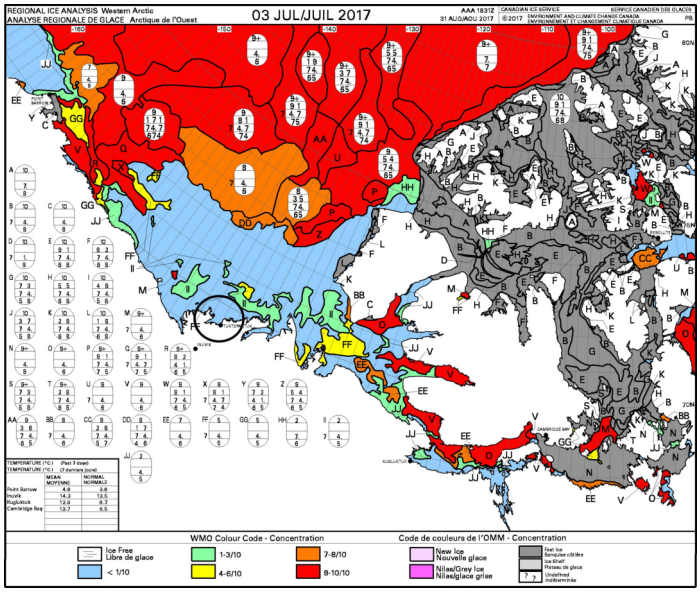
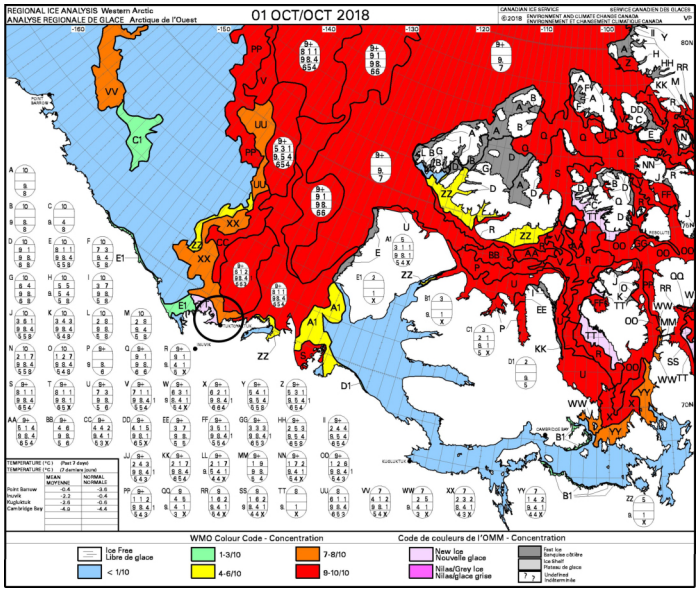
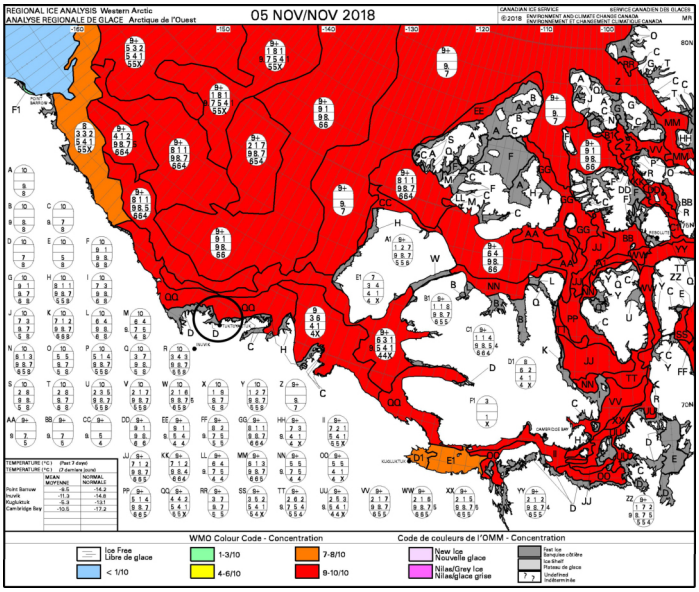


Figure S3. Sea ice charts for the dates listed in Table 2, showing New Ice, Fast Ice, and Ice Free conditions. Tuktoyaktuk is marked by a circle. Sea ice concentration is shown using standard WMO nomenclature and color coding.

New Ice



Fast Ice



Ice Free

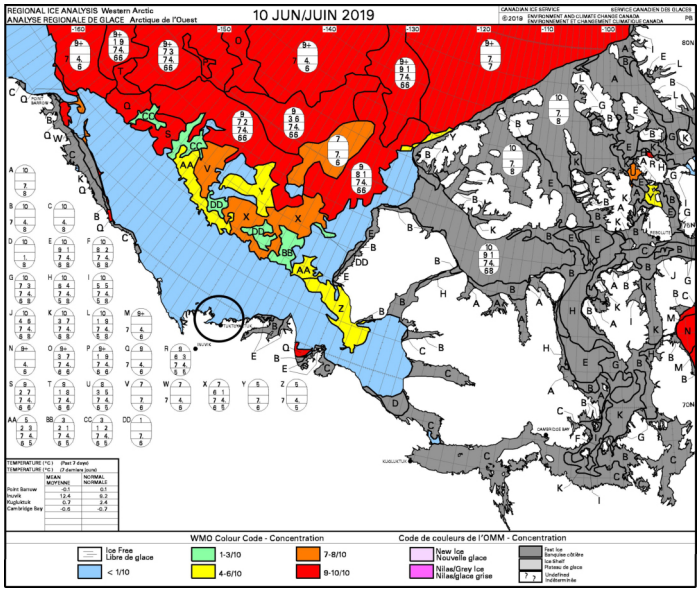
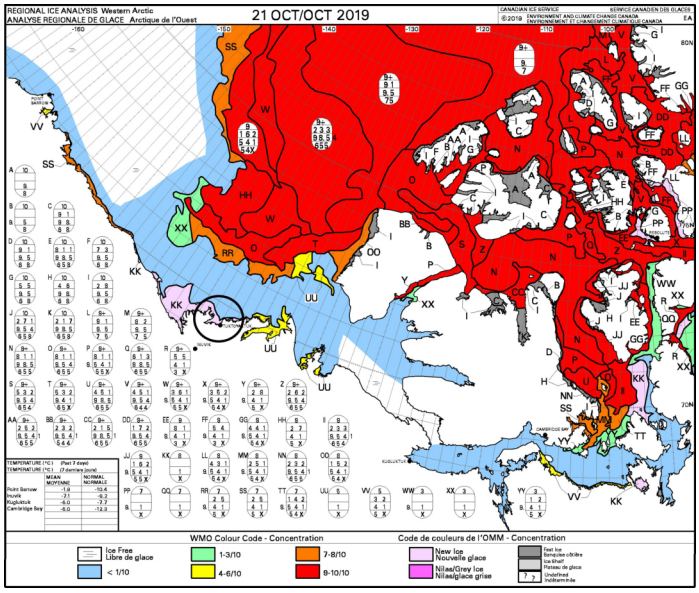
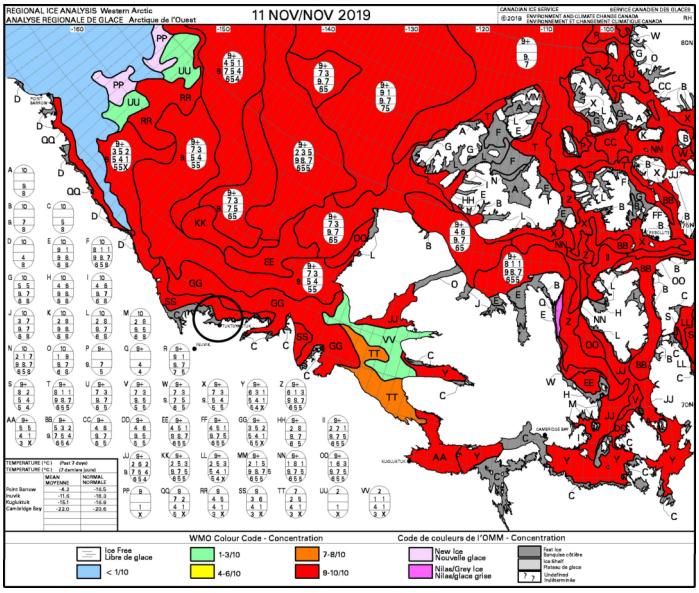


Figure S3. Sea ice charts (continued): 2018–2019 ice season.

New Ice



Fast Ice



Ice Free

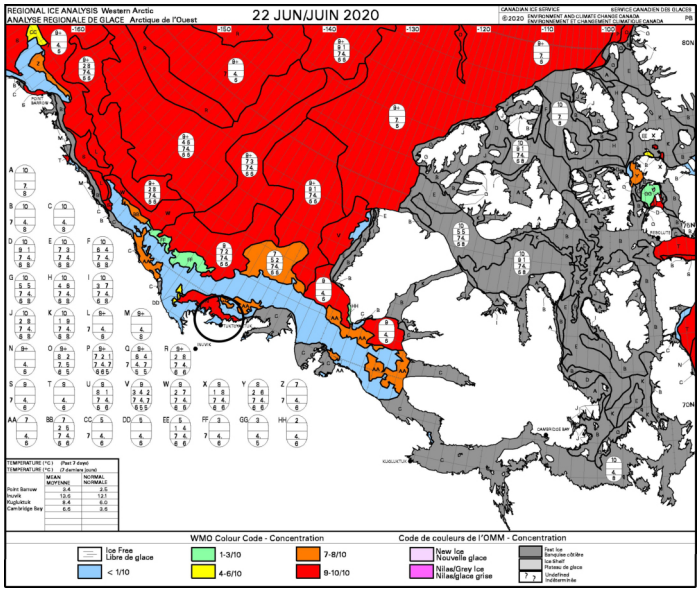
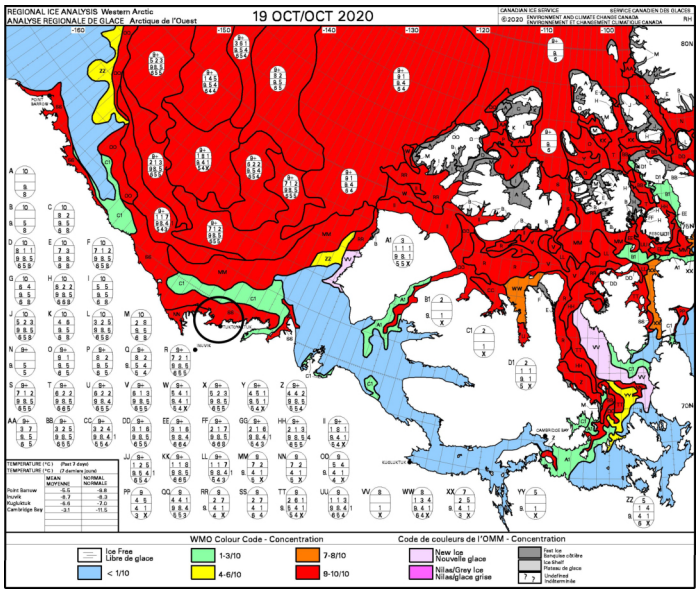
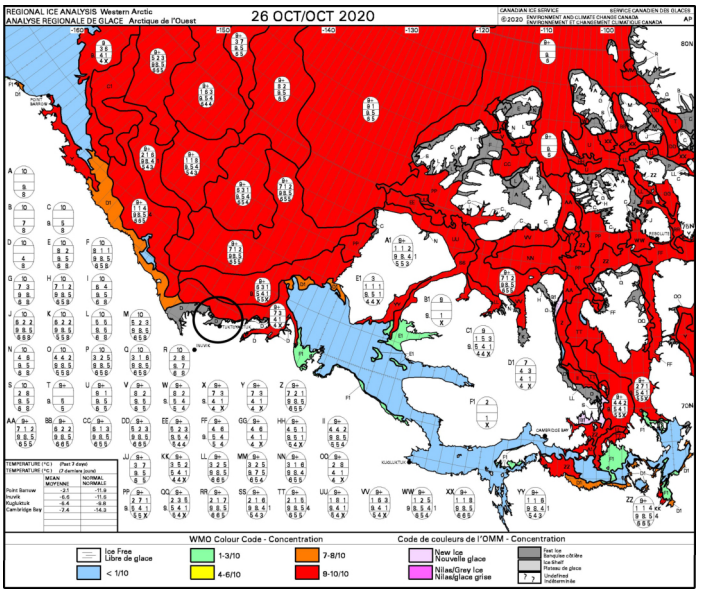


Figure S3. Sea ice charts (continued): 2019–2020 ice season.

New Ice



Fast Ice



Ice Free

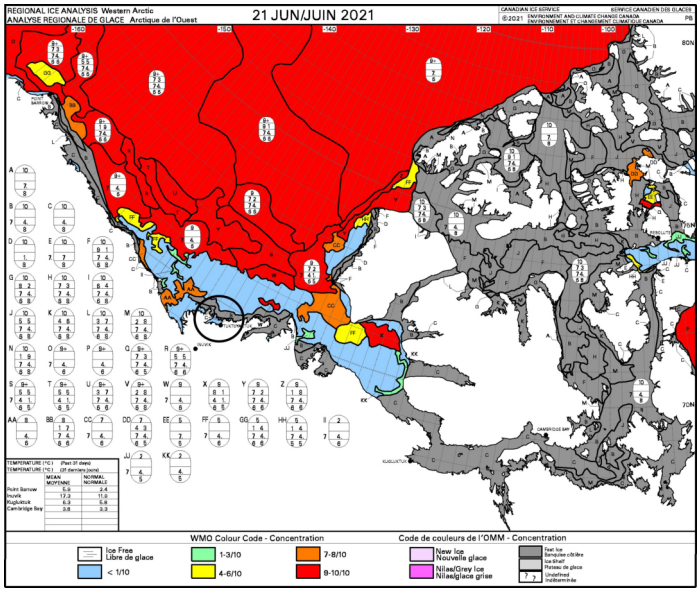
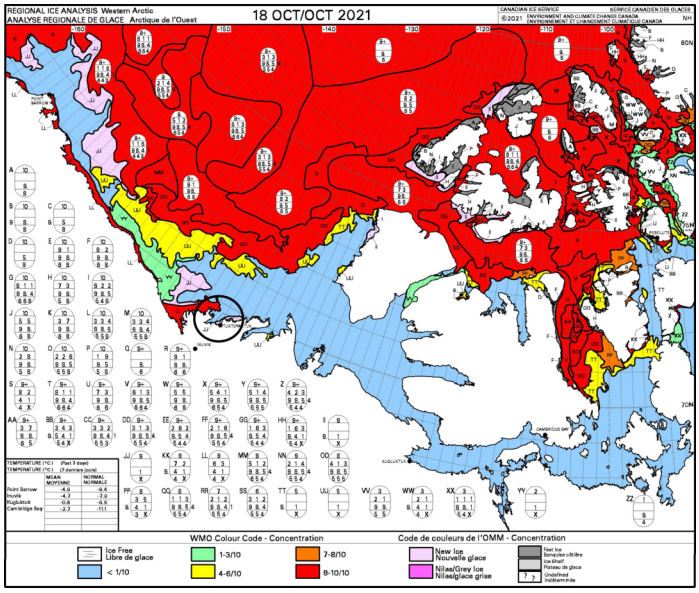
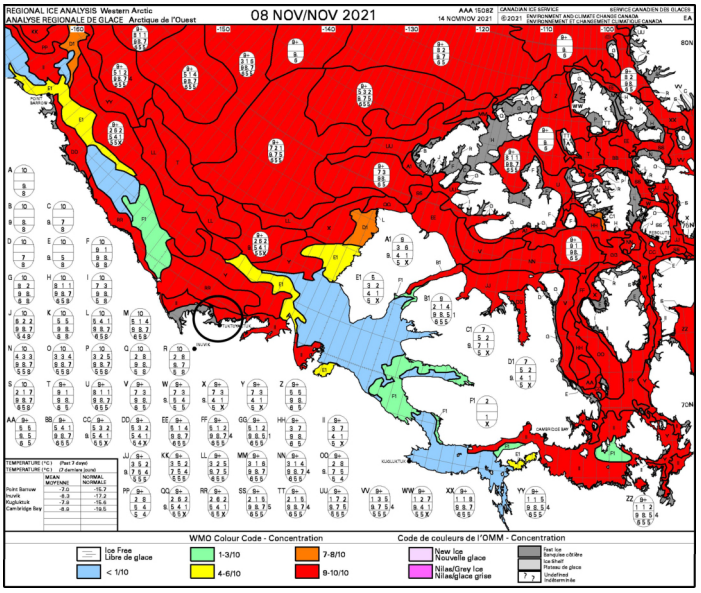


Figure S3. Sea ice charts (continued): 2020–2021 ice season.

New Ice



Fast Ice



Ice Free

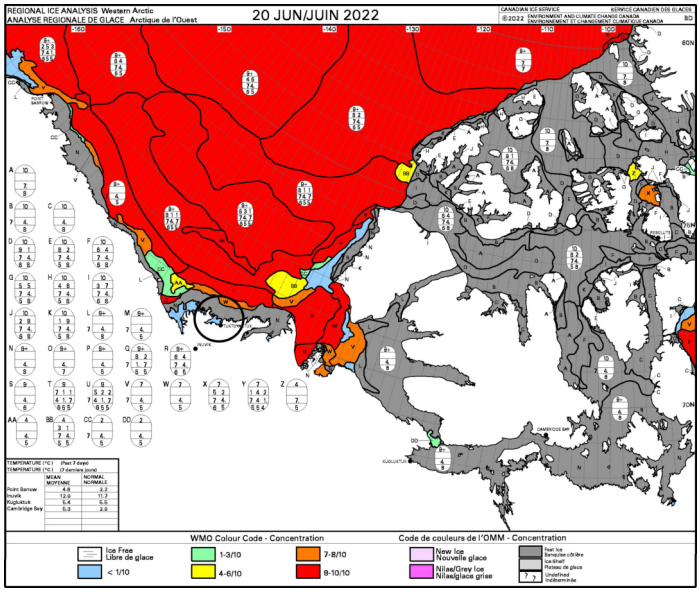
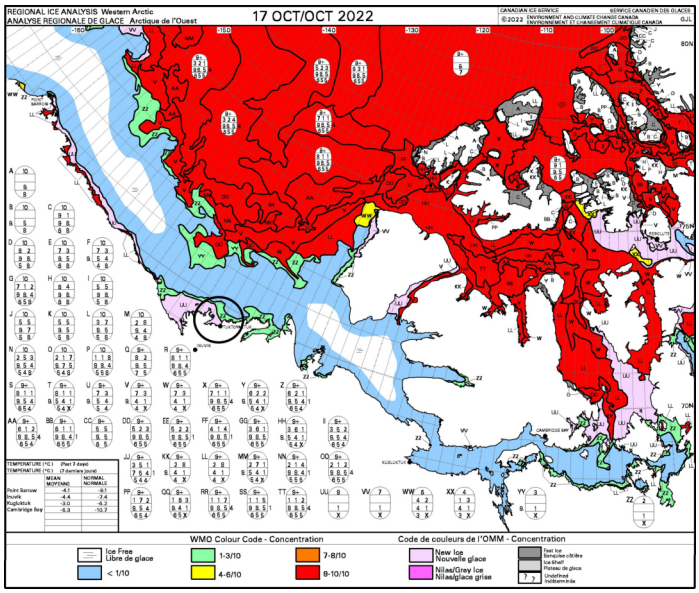
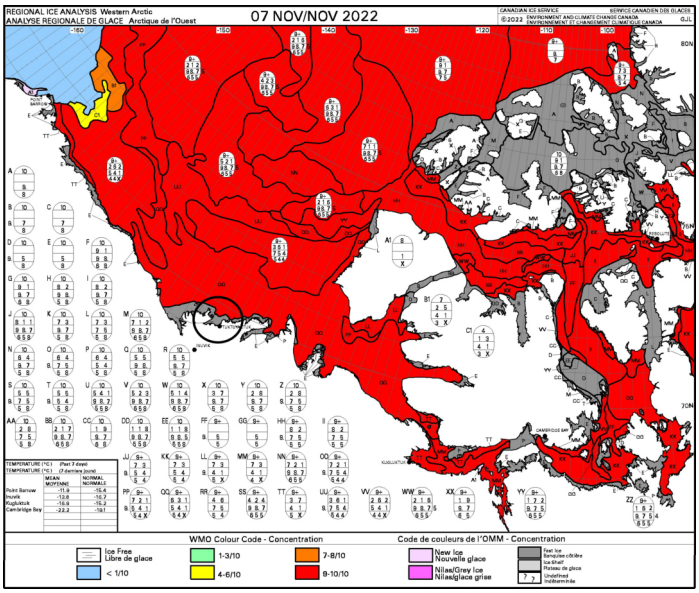


Figure S3. Sea ice charts (continued): 2021–2022 ice season.

New Ice



Fast Ice



Ice Free

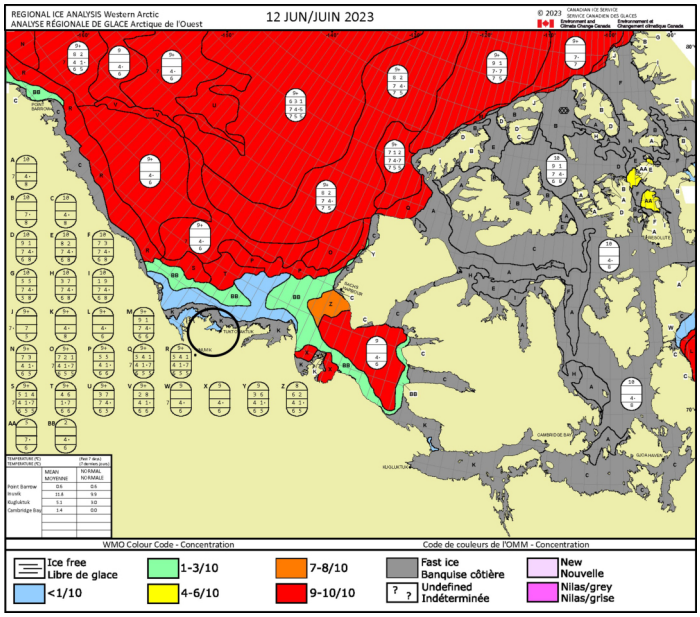


Figure S3. Sea ice charts (continued): 2022–2023 ice season.

SAR results

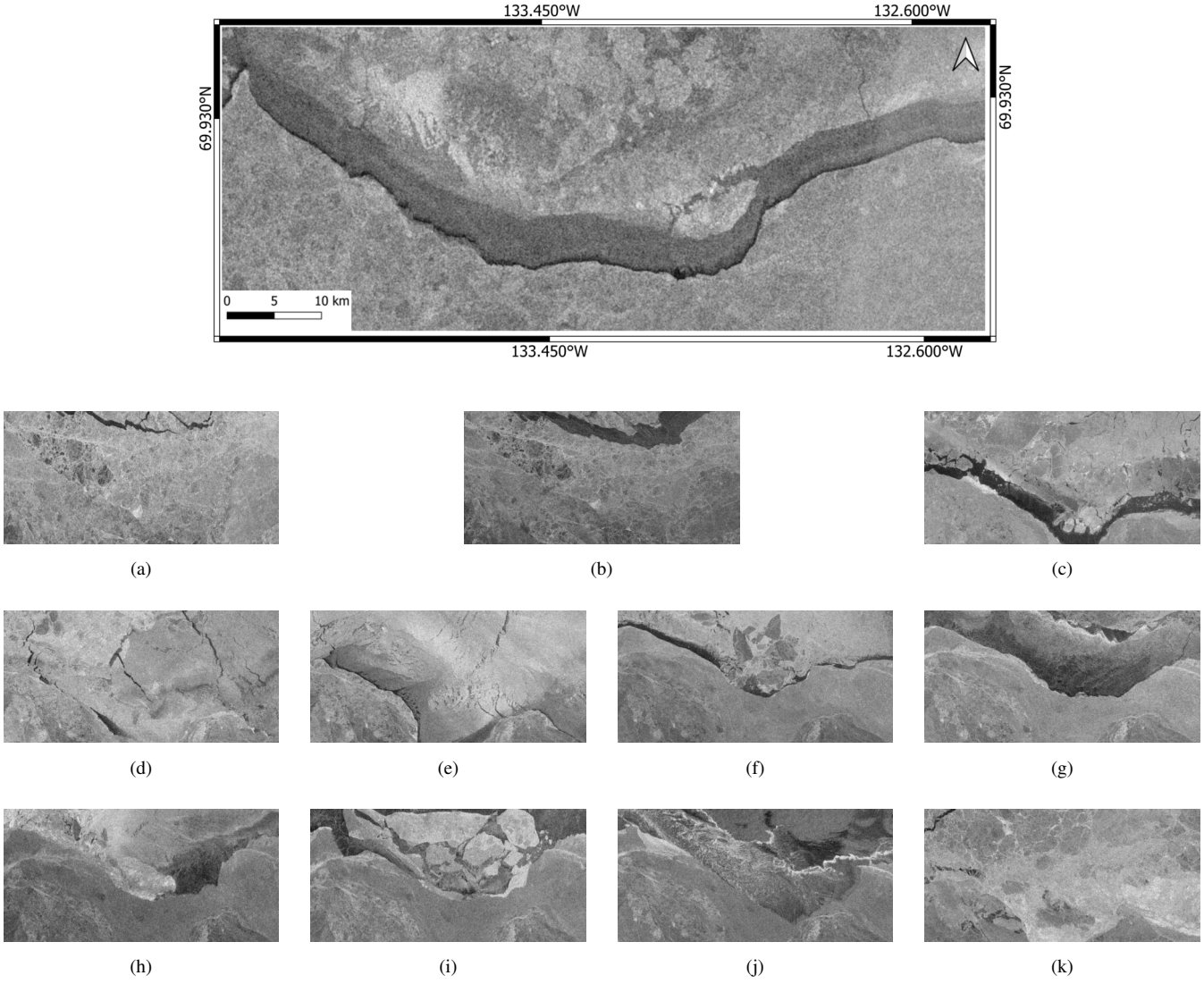
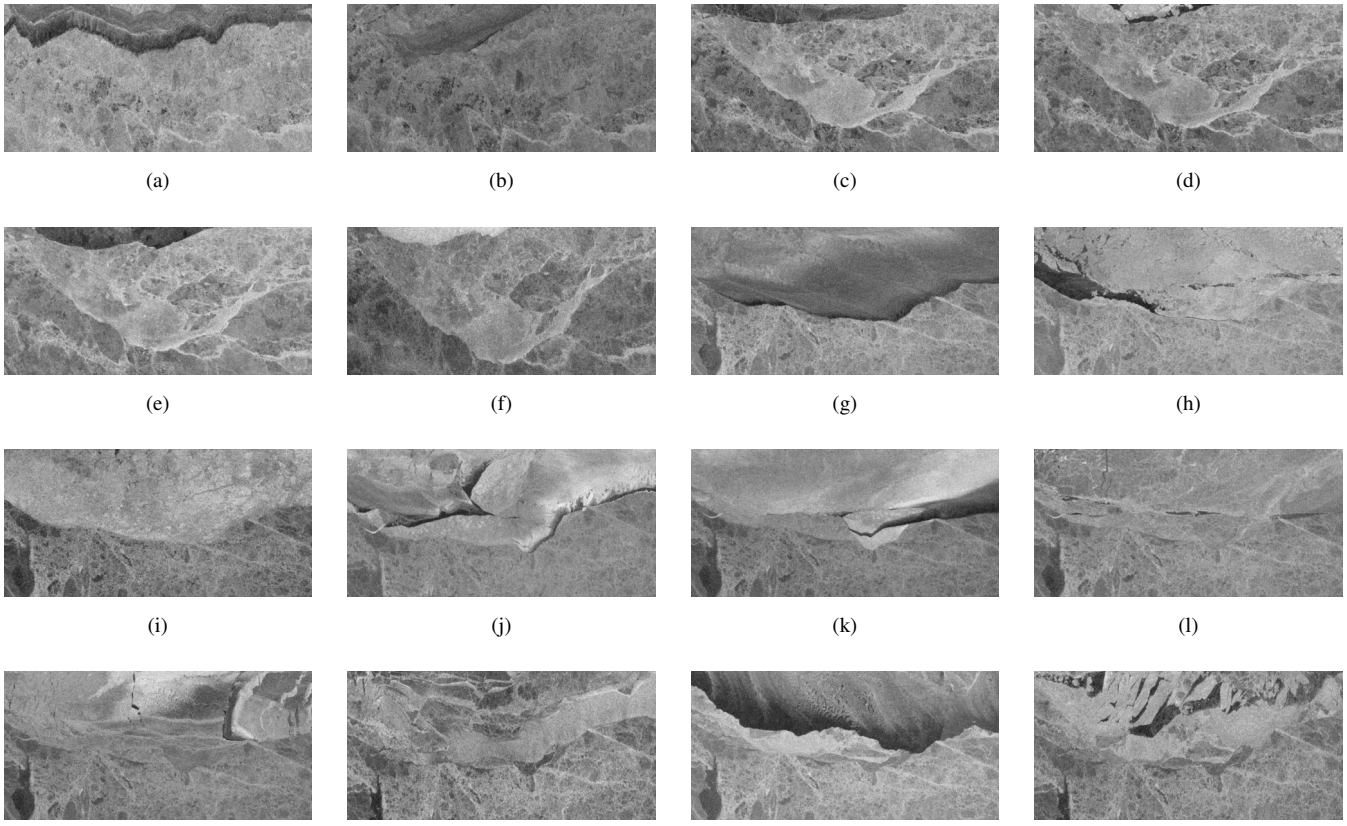


Figure S4. Pre-processing results for Sentinel-1 SAR imagery used in the fracture analysis. The panels show the processed SAR backscatter imagery at 40 m × 40 m pixel spacing and the corresponding threshold-based outputs derived using 500 m × 500 m and 1 km × 1 km spatial windows. A representative SAR image is shown at a larger size with geographic coordinates and a scale bar; the same spatial extent and scale apply to all remaining sub-figures. The results illustrate the identification and spatial representation of low-backscatter fracture features. Sub-figures correspond to SAR acquisitions on the following dates: (a) 2017-02-11, (b) 2017-02-13, (c) 2018-12-05, (d) 2018-12-17, (e) 2018-12-29, (f) 2019-02-10, (g) 2019-03-06, (h) 2019-03-16, (i) 2019-04-21, (j) 2019-05-05, and (k) 2019-12-07.



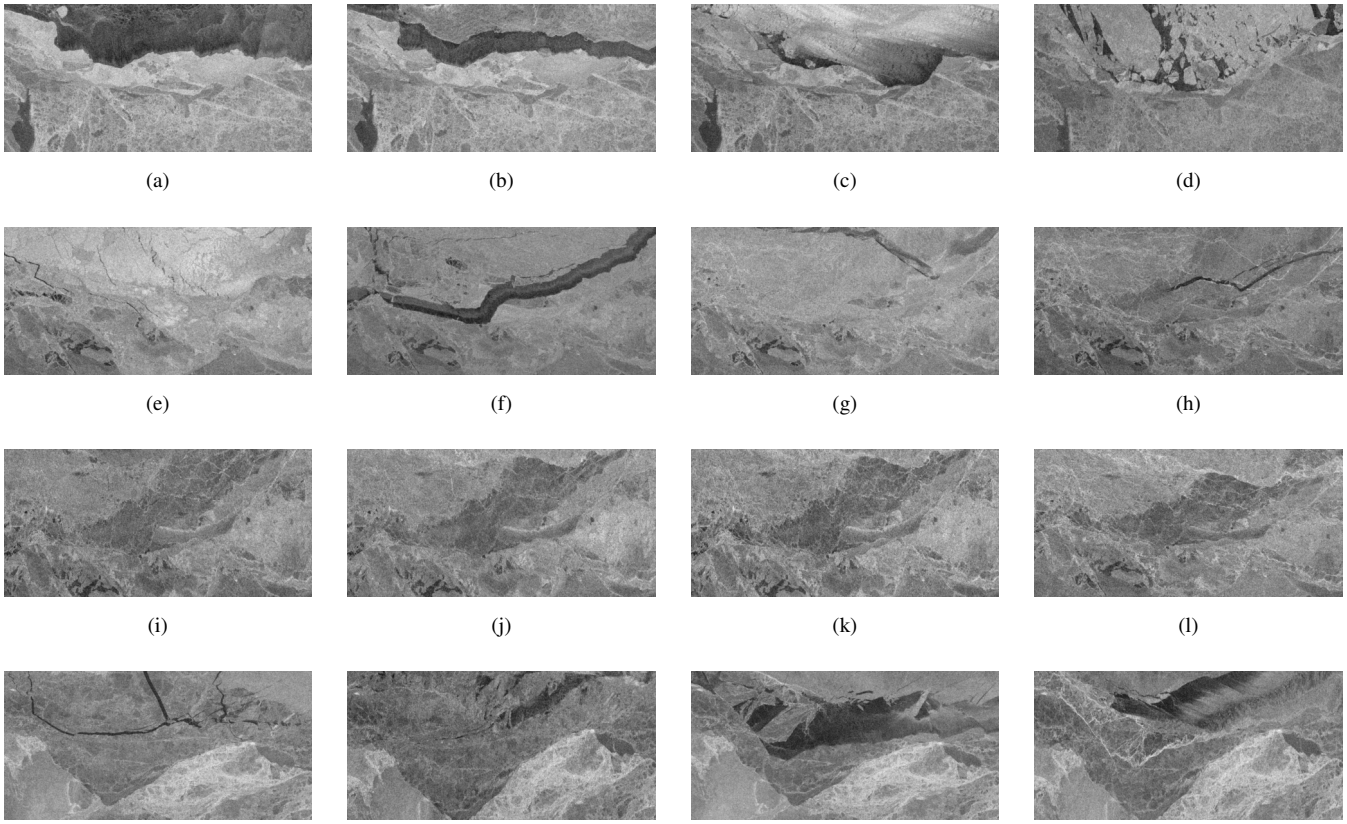
(a) (b) (c) (d)

(e) (f) (g) (h)

(i) (j) (k) (l)

(m) (n) (o) (p)

Figure S5. Continued from Figure S4 of SAR imagery pre-processing results. These sub-figures highlight additional temporal coverage of sea ice backscatter and fracture features. Sub-figures correspond to SAR acquisitions on the following dates: (a) 2021-12-06, (b) 2021-12-18, (c) 2022-02-23, (d) 2022-04-07, (e) 2022-04-24, (f) 2022-05-09, (g) 2022-12-08, (h) 2022-12-15, (i) 2023-01-01, (j) 2023-01-04, (k) 2023-01-08, (l) 2023-01-13, (m) 2023-01-20, (n) 2023-02-23, (o) 2023-03-09, and (p) 2023-03-19.



(a) (b) (c) (d)

(e) (f) (g) (h)

(i) (j) (k) (l)

(m) (n) (o) (p)

Figure S6. Continued from Figure S4 of SAR imagery preprocessing results. These sub-figures highlight additional temporal coverage of sea ice backscatter and fracture features. Sub-figures correspond to SAR acquisitions on the following dates: (a) 2023-03-21, (b) 2023-03-26, (c) 2023-04-02, (d) 2023-05-04, (e) 2019-12-19, (f) 2020-01-17, (g) 2020-02-05, (h) 2020-02-17, (i) 2020-03-08, (j) 2020-03-20, (k) 2020-04-01, (l) 2020-04-17, (m) 2021-01-06, (n) 2021-01-16, (o) 2021-02-11, and (p) 2021-03-05.

565 **Wind and Temperature analysis**

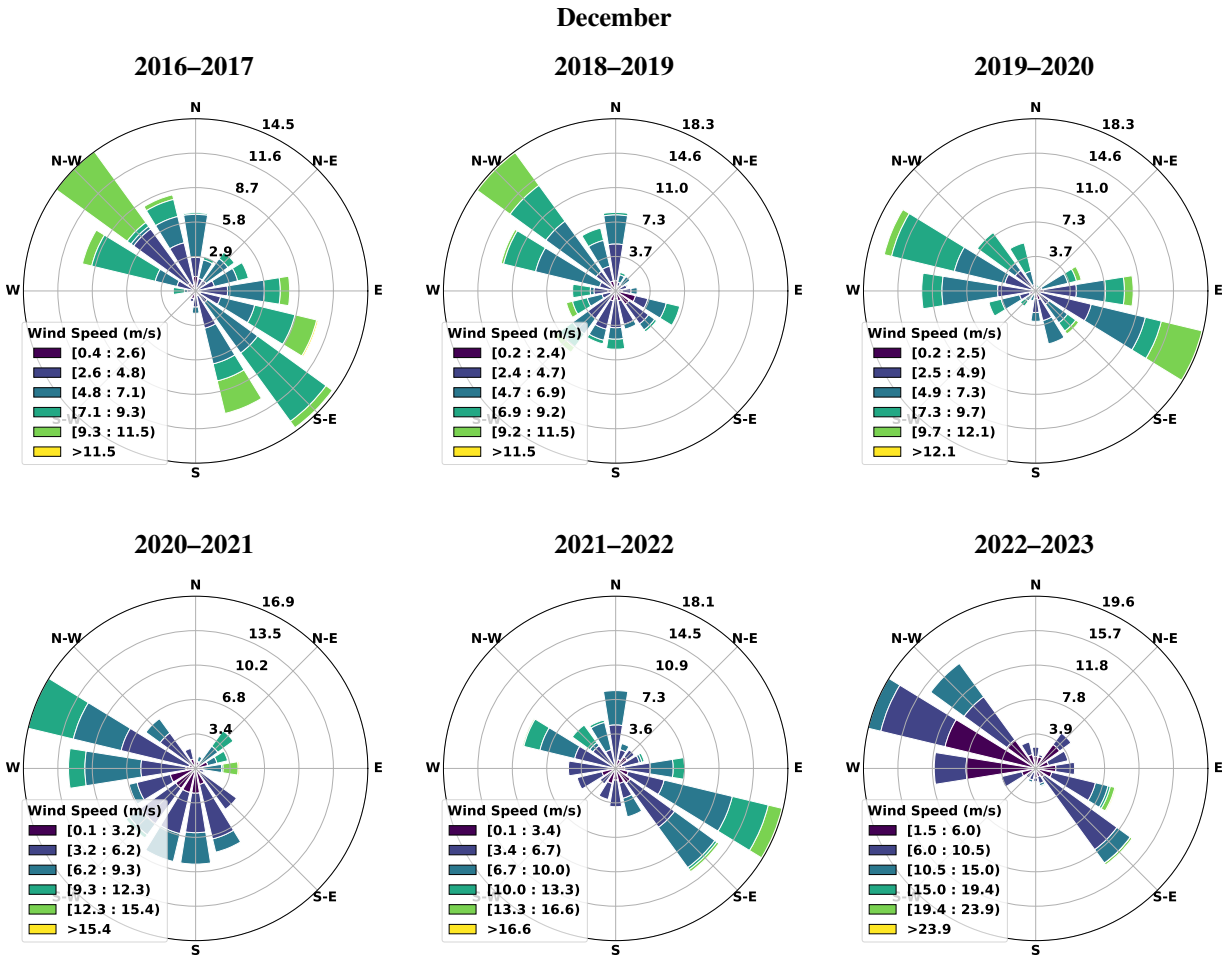


Figure S7. Wind rose plots showing monthly mean wind speed and direction from December through May for each analyzed ice season. The radial spokes indicate the direction from which the wind originates, and the colors represent different wind-speed ranges. Overall, winds near the Tuktoyaktuk LFSI area exhibit substantial seasonal variability, with dominant W to E winds from December to March and stronger southwesterly winds during April and May.

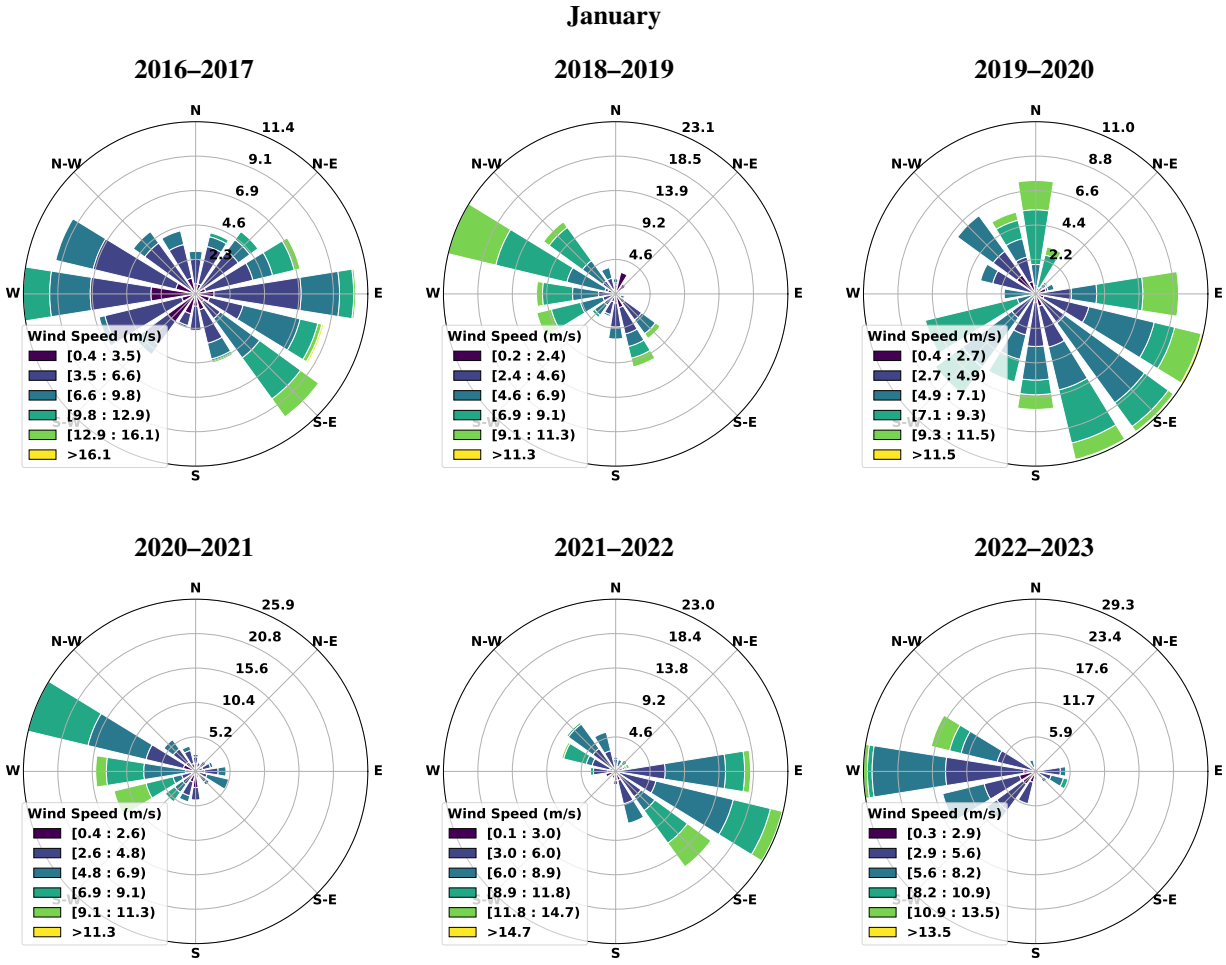


Figure S7. Wind rose plots (continued): January.

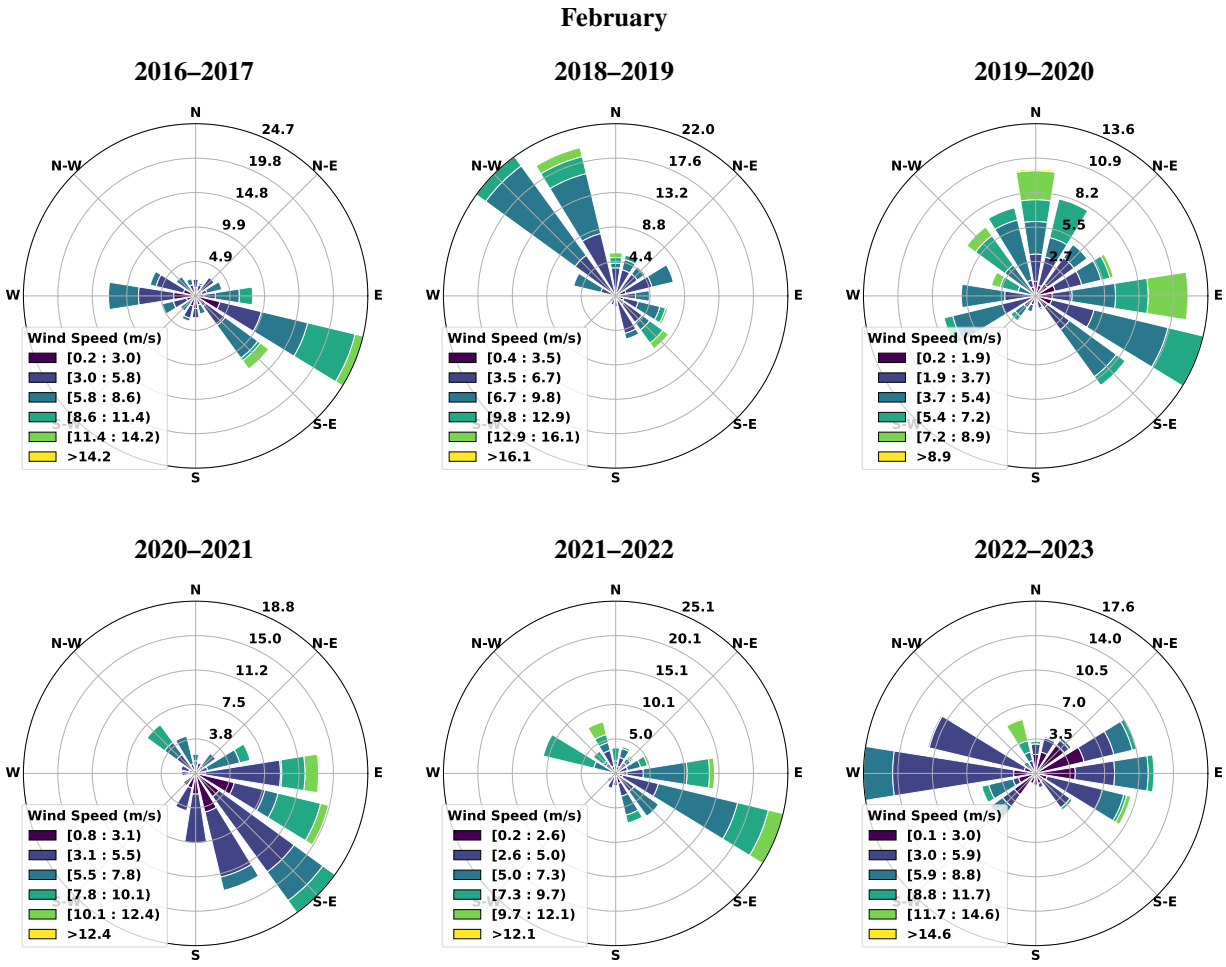


Figure S7. Wind rose plots (continued): February.

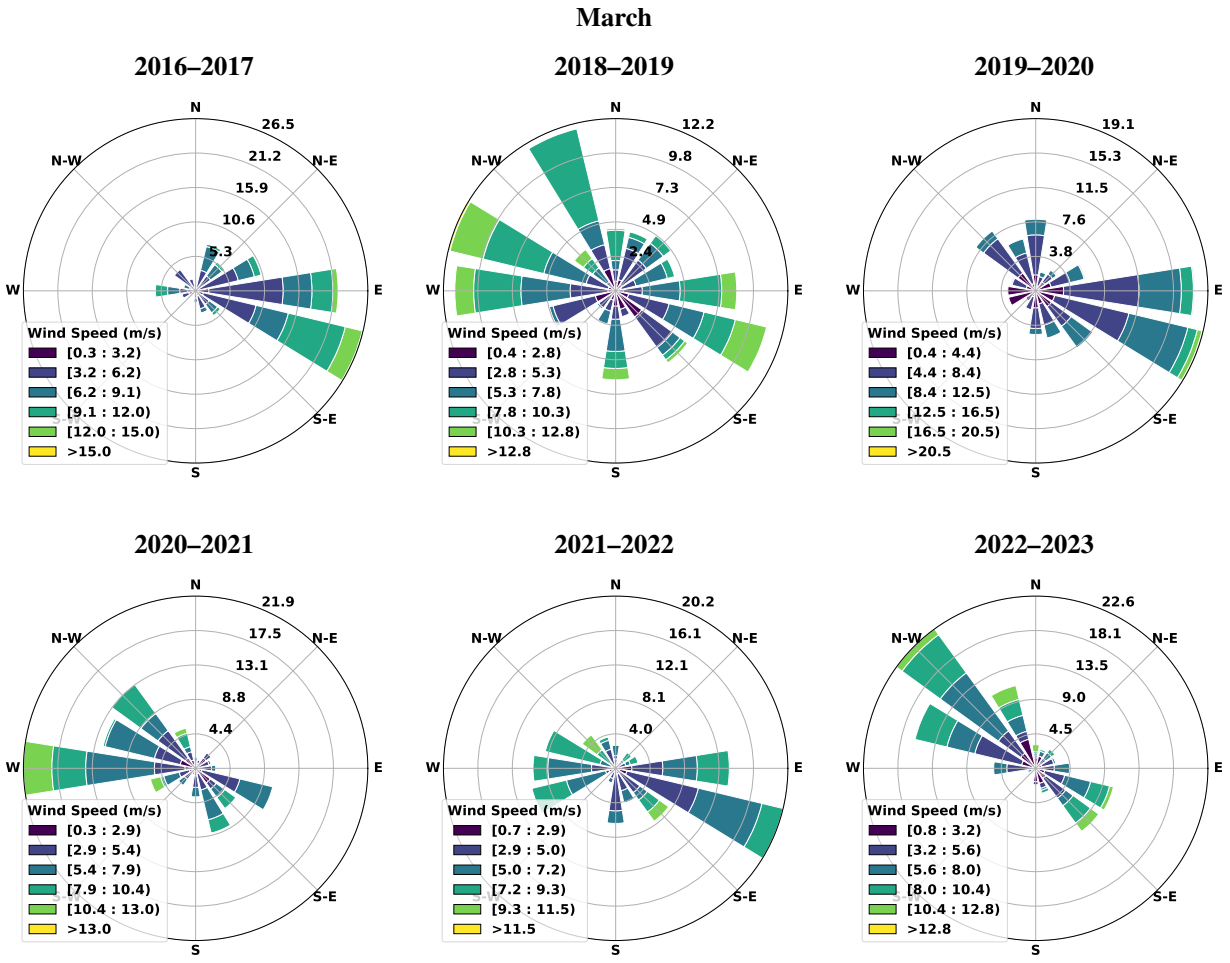


Figure S7. Wind rose plots (continued): March.

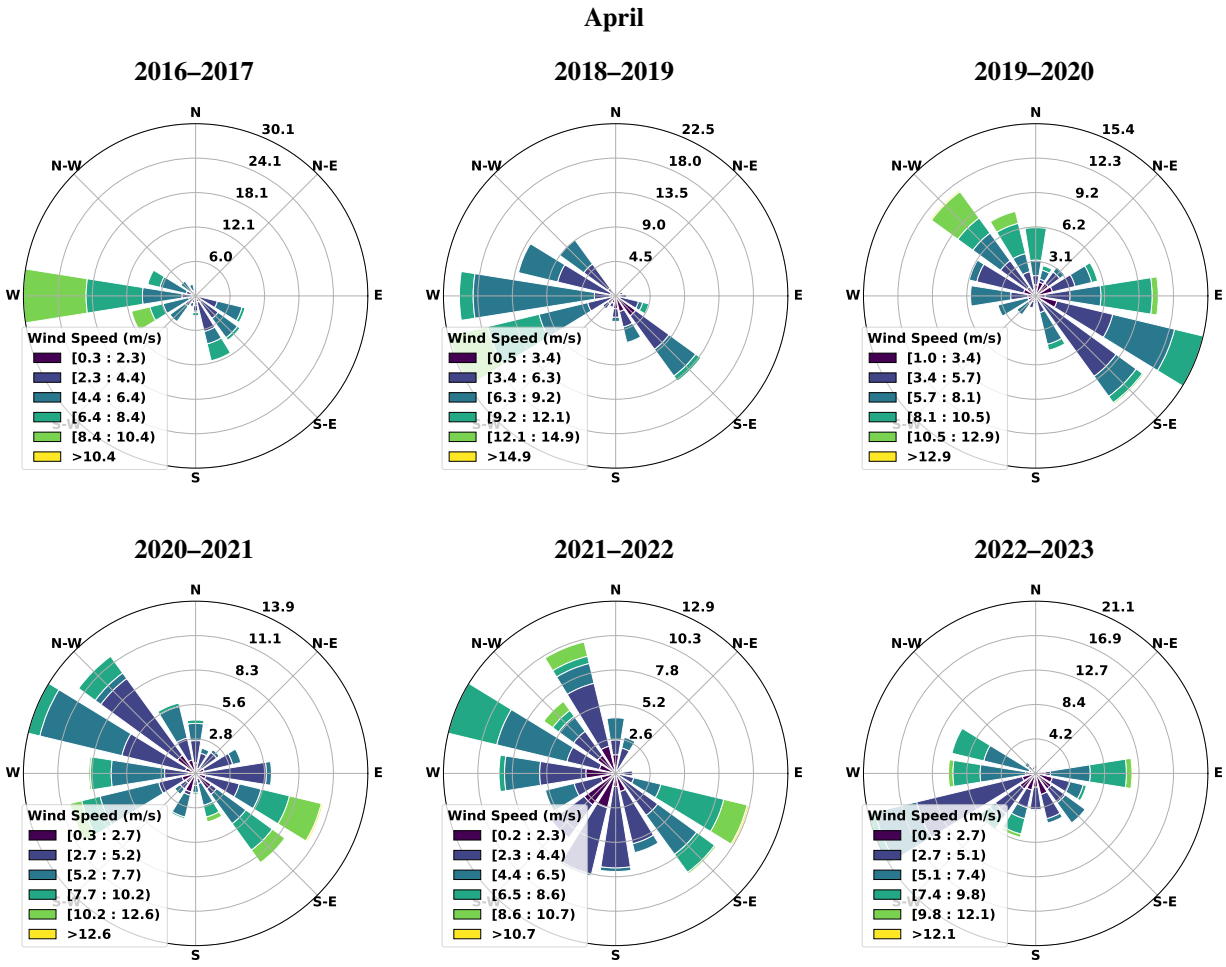


Figure S7. Wind rose plots (continued): April.

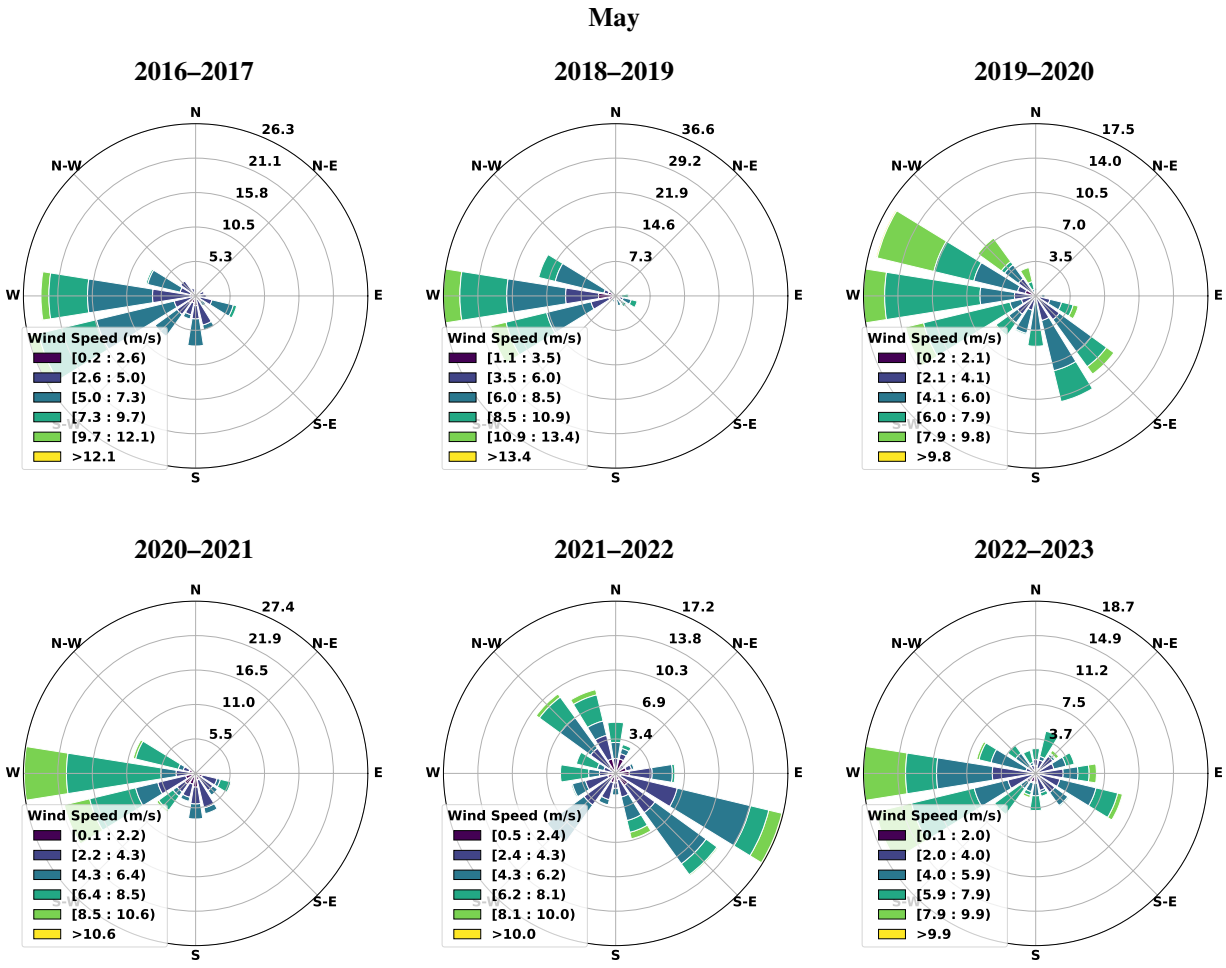


Figure S7. Wind rose plots (continued): May.

Table S1: The average wind speed (km h^{-1}) and temperature (°C), along with the percentage distribution of wind originating from land (L: E, ESE, SE, SSE, S, SSW, SW, WSW, and W) and ocean (O: WNW, NW, NNW, N, NNE, NE, and ENE). WS: Wind Speed, WD (L, O): Wind Direction (Land, Ocean), T: Temperature. The 7-, 3-, 2-, and 1-day columns represent averages over the respective periods preceding each midpoint-based nominal fracture date, whereas On the Day represents conditions on the nominal fracture date.

Dates	7 Days			3 Days			2 Days		
	WS	WD (L,O)	T	WS	WD (L,O)	T	WS	WD (L,O)	T
2016-12-19	20.26	(67.26, 32.74)	-23.00	23.32	(100.00, 0.00)	-25.19	23.84	(100.00, 0.00)	-24.69
2017-02-08	20.96	(29.17, 70.83)	-11.99	14.51	(23.61, 76.39)	-13.84	15.11	(35.42, 64.58)	-15.57

Continued on next page

Table S1 – continued

Dates	7 Days			3 Days			2 Days		
	WS	WD (L,O)	T	WS	WD (L,O)	T	WS	WD (L,O)	T
2017-02-12	18.77	(35.71, 64.29)	-21.72	18.71	(45.83, 54.17)	-31.00	15.57	(58.33, 41.67)	-34.53
2018-11-29	15.68	(50.00, 50.00)	-13.63	17.10	(45.83, 54.17)	-18.45	14.43	(68.75, 31.25)	-12.15
2018-12-15	18.72	(42.86, 57.14)	-19.47	21.85	(68.06, 31.94)	-20.60	18.76	(100.00, 0.00)	-20.17
2018-12-27	10.99	(51.79, 48.21)	-23.95	15.70	(51.39, 48.61)	-31.47	17.20	(77.08, 22.92)	-33.00
2019-02-08	19.90	(91.07, 8.93)	-24.61	21.01	(100.00, 0.00)	-21.10	22.64	(100.00, 0.00)	-22.34
2019-03-04	21.81	(86.31, 13.69)	-16.00	27.19	(100.00, 0.00)	-18.00	27.41	(100.00, 0.00)	-17.09
2019-03-15	15.23	(54.76, 45.24)	-16.24	15.67	(33.33, 66.67)	-23.84	15.48	(50.00, 50.00)	-24.47
2019-04-20	22.64	(67.86, 32.14)	-11.64	20.14	(70.83, 29.17)	-11.11	21.75	(56.25, 43.75)	-11.12
2019-05-04	16.58	(50.60, 49.40)	-8.63	24.17	(55.56, 44.44)	-8.38	24.17	(77.08, 22.92)	-11.21
2019-12-06	19.39	(34.17, 65.83)	-19.98	21.30	(20.83, 79.17)	-21.90	25.03	(31.25, 68.75)	-21.39
2019-12-18	15.33	(93.45, 6.55)	-25.64	10.88	(84.72, 15.28)	-27.87	10.64	(77.08, 22.92)	-28.62
2020-01-15	19.71	(59.52, 40.48)	-25.86	18.74	(95.83, 4.17)	-25.80	22.27	(100.00, 0.00)	-23.73
2020-02-04	14.03	(45.83, 54.17)	-31.60	13.72	(100.00, 0.00)	-34.25	16.65	(100.00, 0.00)	-34.81
2020-02-16	12.50	(76.79, 23.21)	-33.97	10.79	(77.78, 22.22)	-36.73	10.39	(100.00, 0.00)	-36.75
2020-03-07	14.26	(67.26, 32.74)	-34.00	14.82	(81.94, 18.06)	-34.11	16.68	(81.25, 18.75)	-32.73
2020-03-19	26.67	(64.29, 35.71)	-16.70	21.91	(62.50, 37.50)	-15.20	23.07	(56.25, 43.75)	-13.14
2020-03-31	20.96	(44.05, 55.95)	-22.27	17.42	(68.06, 31.94)	-26.73	14.77	(64.58, 35.42)	-26.92
2020-04-16	13.80	(76.79, 23.21)	-10.62	13.54	(81.94, 18.06)	-5.27	14.23	(72.92, 27.08)	-4.81
2021-01-05	13.53	(43.45, 56.55)	-26.70	16.46	(61.11, 38.89)	-27.79	14.30	(41.67, 58.33)	-26.87
2021-01-15	16.06	(47.62, 52.38)	-18.77	15.44	(8.33, 91.67)	-21.36	9.94	(12.50, 87.50)	-23.77
2021-02-10	14.66	(53.57, 46.43)	-34.13	13.99	(41.67, 58.33)	-34.03	9.49	(62.50, 37.50)	-36.98
2021-03-04	13.89	(66.67, 33.33)	-35.17	13.62	(75.00, 25.00)	-33.20	14.96	(79.17, 20.83)	-31.09
2021-12-04	13.51	(55.56, 44.44)	-29.53	13.51	(55.56, 44.44)	-29.53	17.93	(33.33, 66.67)	-28.25
2021-12-17	14.75	(37.50, 62.50)	-25.32	10.57	(54.17, 45.83)	-30.25	12.54	(52.08, 47.92)	-31.41
2022-01-22	12.82	(80.36, 19.64)	-32.49	15.43	(56.94, 43.06)	-29.36	17.90	(64.58, 35.42)	-30.72
2022-02-21	15.79	(66.07, 33.93)	-29.06	12.56	(50.00, 50.00)	-27.15	12.60	(31.25, 68.75)	-29.67
2022-02-27	17.04	(65.48, 34.52)	-24.22	14.45	(37.50, 62.50)	-26.03	12.36	(43.75, 56.25)	-28.85
2022-04-05	10.83	(2.98, 97.02)	-27.41	8.18	(0.00, 100.00)	-26.91	7.01	(0.00, 100.00)	-26.49
2022-04-22	9.77	(57.14, 42.86)	-15.73	9.55	(41.67, 58.33)	-13.50	7.90	(12.50, 87.50)	-15.50
2022-04-29	13.60	(51.19, 48.81)	-9.09	10.40	(18.06, 81.94)	-11.00	10.35	(27.08, 72.92)	-11.93
2022-05-08	15.74	(63.69, 36.31)	-0.25	15.75	(59.72, 40.28)	-2.22	14.10	(89.58, 10.42)	-1.75
2022-12-06	25.79	(59.17, 40.83)	-17.42	33.12	(66.67, 33.33)	-17.23	25.30	(68.75, 31.25)	-23.57
2022-12-13	19.31	(100.00, 0.00)	-26.13	20.78	(100.00, 0.00)	-22.38	23.02	(100.00, 0.00)	-23.12
2022-12-30	15.02	(72.62, 27.38)	-30.96	14.14	(65.28, 34.72)	-27.57	13.23	(87.50, 12.50)	-26.13
2023-01-03	16.55	(85.12, 14.88)	-23.45	20.18	(100.00, 0.00)	-20.23	23.33	(100.00, 0.00)	-20.08

Continued on next page

Table S1 – continued

Dates	7 Days			3 Days			2 Days		
	WS	WD (L,O)	T	WS	WD (L,O)	T	WS	WD (L,O)	T
2023-01-06	17.47	(98.21, 1.79)	-18.85	16.28	(95.83, 4.17)	-16.84	12.07	(93.75, 6.25)	-17.43
2023-01-11	13.35	(67.86, 32.14)	-20.82	13.62	(73.61, 26.39)	-21.67	15.65	(60.42, 39.58)	-21.30
2023-01-18	13.81	(78.57, 21.43)	-26.14	10.89	(80.56, 19.44)	-25.16	10.38	(100.00, 0.00)	-25.18
2023-02-22	13.50	(94.05, 5.95)	-33.21	14.08	(86.11, 13.89)	-30.25	13.93	(79.17, 20.83)	-28.94
2023-02-24	16.24	(89.29, 10.71)	-31.31	21.50	(75.00, 25.00)	-27.41	23.45	(83.33, 16.67)	-27.99
2023-03-08	11.61	(69.05, 30.95)	-32.03	12.18	(100.00, 0.00)	-31.81	14.09	(100.00, 0.00)	-30.52
2023-03-18	12.90	(74.40, 25.60)	-26.67	8.53	(84.72, 15.28)	-32.40	8.53	(100.00, 0.00)	-32.61
2023-03-20	12.97	(78.57, 21.43)	-27.31	13.51	(100.00, 0.00)	-24.91	15.17	(100.00, 0.00)	-21.38
2023-03-24	16.28	(100.00, 0.00)	-15.89	18.01	(100.00, 0.00)	-9.26	18.02	(100.00, 0.00)	-9.93
2023-04-01	20.78	(72.02, 27.98)	-12.83	19.93	(86.11, 13.89)	-17.87	21.56	(100.00, 0.00)	-18.90
2023-05-03	14.31	(47.62, 52.38)	-10.46	15.43	(41.67, 58.33)	-7.54	14.44	(62.50, 37.50)	-5.37

Table S2: Table S1 continued: 1-day averages and conditions on the midpoint-based nominal fracture date.

Dates	1 Day			On the Day		
	WS	WD (L,O)	T	WS	WD (L,O)	T
2016-12-19	26.27	(100.00, 0.00)	-24.89	28.03	(100.00, 0.00)	-23.88
2017-02-08	17.66	(58.33, 41.67)	-16.42	31.76	(41.67, 58.33)	-17.50
2017-02-12	15.07	(100.00, 0.00)	-37.38	15.52	(100.00, 0.00)	-36.44
2018-11-29	13.40	(100.00, 0.00)	-11.17	9.30	(100.00, 0.00)	-12.07
2018-12-15	18.56	(100.00, 0.00)	-20.74	19.48	(100.00, 0.00)	-24.42
2018-12-27	22.58	(100.00, 0.00)	-31.84	31.31	(100.00, 0.00)	-26.13
2019-02-08	25.09	(100.00, 0.00)	-25.51	39.92	(100.00, 0.00)	-15.73
2019-03-04	27.21	(100.00, 0.00)	-14.64	18.94	(62.50, 37.50)	-8.33
2019-03-15	23.55	(100.00, 0.00)	-25.30	21.79	(100.00, 0.00)	-16.38
2019-04-20	23.99	(33.33, 66.67)	-12.04	19.79	(87.50, 12.50)	-8.78
2019-05-04	20.94	(100.00, 0.00)	-9.72	19.27	(58.33, 41.67)	-7.56
2019-12-06	30.54	(8.33, 91.67)	-18.34	25.34	(0.00, 100.00)	-16.94
2019-12-18	12.61	(62.50, 37.50)	-29.00	9.71	(100.00, 0.00)	-31.54
2020-01-15	21.13	(100.00, 0.00)	-24.16	30.31	(54.17, 45.83)	-15.85
2020-02-04	14.23	(100.00, 0.00)	-39.43	19.72	(100.00, 0.00)	-31.30
2020-02-16	5.58	(100.00, 0.00)	-38.63	13.35	(100.00, 0.00)	-39.45
2020-03-07	11.85	(100.00, 0.00)	-33.86	21.19	(100.00, 0.00)	-27.42
2020-03-19	23.70	(95.83, 4.17)	-13.43	21.06	(100.00, 0.00)	-5.55

Continued on next page

Table S1 – continued

Dates	1 Day			On the Day		
	WS	WD (L,O)	T	WS	WD (L,O)	T
2020-03-31	14.88	(100.00, 0.00)	-26.25	24.97	(100.00, 0.00)	-18.27
2020-04-16	12.92	(91.67, 8.33)	-3.83	16.89	(29.17, 70.83)	-3.31
2021-01-05	8.80	(83.33, 16.67)	-29.04	13.88	(100.00, 0.00)	-26.35
2021-01-15	3.98	(25.00, 75.00)	-24.25	21.65	(91.67, 8.33)	-27.14
2021-02-10	12.82	(95.83, 4.17)	-37.79	15.95	(100.00, 0.00)	-36.95
2021-03-04	10.51	(66.67, 33.33)	-31.36	13.11	(100.00, 0.00)	-29.64
2021-12-04	20.06	(66.67, 33.33)	-28.61	12.64	(100.00, 0.00)	-31.39
2021-12-17	14.31	(100.00, 0.00)	-33.75	19.72	(100.00, 0.00)	-28.60
2022-01-22	16.55	(100.00, 0.00)	-30.93	22.41	(100.00, 0.00)	-28.61
2022-02-21	14.20	(62.50, 37.50)	-31.42	14.37	(100.00, 0.00)	-31.52
2022-02-27	10.18	(87.50, 12.50)	-30.01	20.32	(100.00, 0.00)	-26.97
2022-04-05	8.34	(0.00, 100.00)	-27.05	8.23	(66.67, 33.33)	-25.65
2022-04-22	7.45	(25.00, 75.00)	-16.79	19.24	(100.00, 0.00)	-13.35
2022-04-29	10.17	(54.17, 45.83)	-12.50	17.58	(100.00, 0.00)	-7.01
2022-05-08	11.80	(100.00, 0.00)	-0.82	20.36	(100.00, 0.00)	1.95
2022-12-06	29.33	(100.00, 0.00)	-26.71	26.60	(100.00, 0.00)	-27.29
2022-12-13	26.54	(100.00, 0.00)	-23.00	23.79	(70.83, 29.17)	-14.67
2022-12-30	13.79	(100.00, 0.00)	-22.09	12.89	(100.00, 0.00)	-20.78
2023-01-03	30.13	(100.00, 0.00)	-19.96	24.69	(100.00, 0.00)	-15.67
2023-01-06	13.27	(87.50, 12.50)	-19.65	14.30	(16.67, 83.33)	-22.98
2023-01-11	18.68	(20.83, 79.17)	-23.79	13.31	(58.33, 41.67)	-29.18
2023-01-18	11.75	(100.00, 0.00)	-22.53	10.98	(62.50, 37.50)	-17.89
2023-02-22	17.60	(58.33, 41.67)	-26.25	13.83	(66.67, 33.33)	-32.58
2023-02-24	33.07	(100.00, 0.00)	-23.39	31.26	(79.17, 20.83)	-10.81
2023-03-08	18.83	(100.00, 0.00)	-29.23	31.56	(100.00, 0.00)	-20.44
2023-03-18	10.19	(100.00, 0.00)	-31.97	12.37	(100.00, 0.00)	-26.28
2023-03-20	17.98	(100.00, 0.00)	-16.48	19.37	(100.00, 0.00)	-8.71
2023-03-24	21.28	(100.00, 0.00)	-10.17	23.23	(100.00, 0.00)	-10.43
2023-04-01	24.48	(100.00, 0.00)	-19.21	20.57	(100.00, 0.00)	-20.28
2023-05-03	9.59	(100.00, 0.00)	-4.00	12.68	(50.00, 50.00)	-1.83

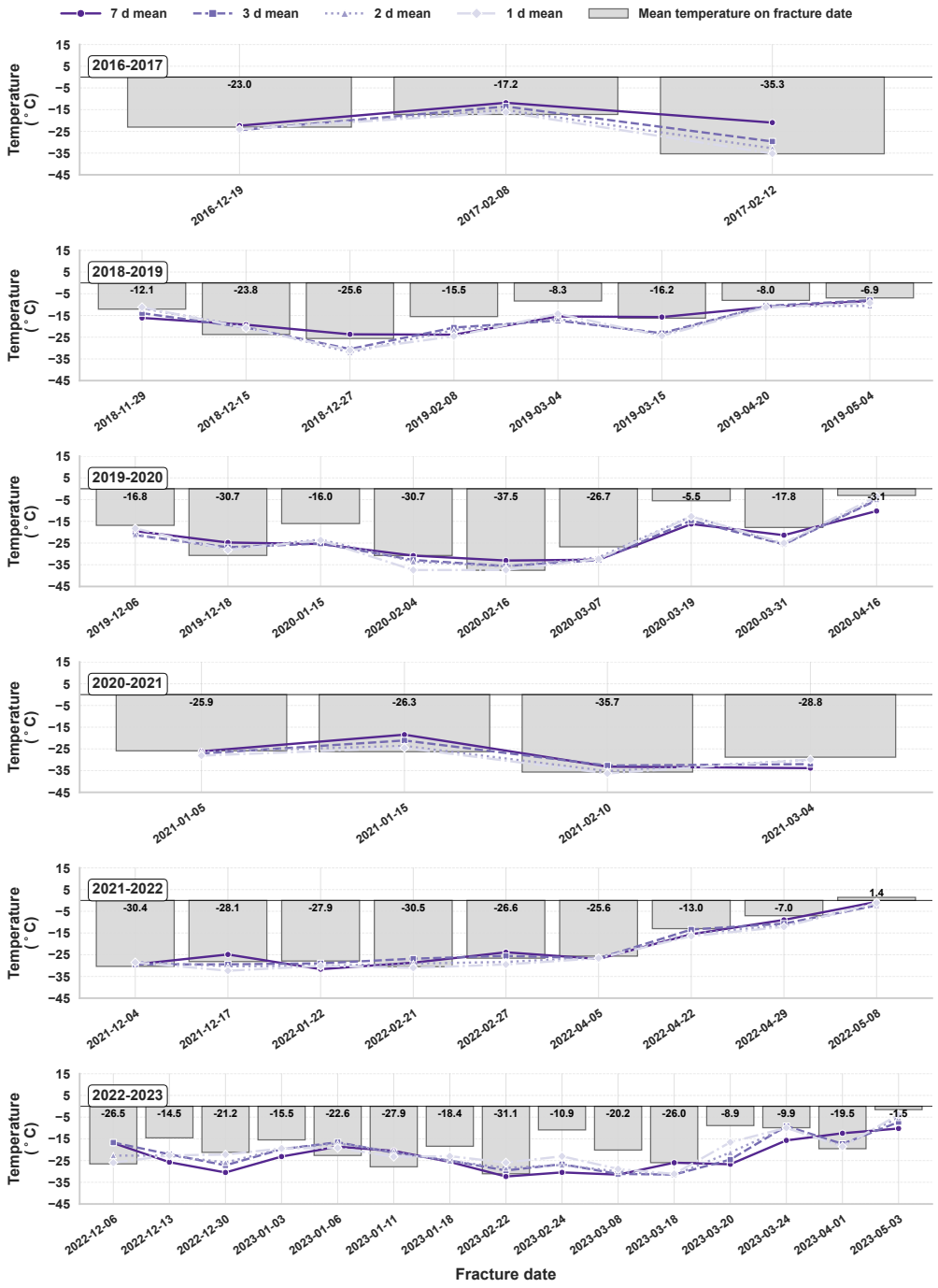


Figure S8. ERA5 temperature on the midpoint-based nominal fracture dates and during the preceding 7, 3, 2, and 1 days. Dates correspond to the nominal fracture dates defined from SAR interval-censoring.

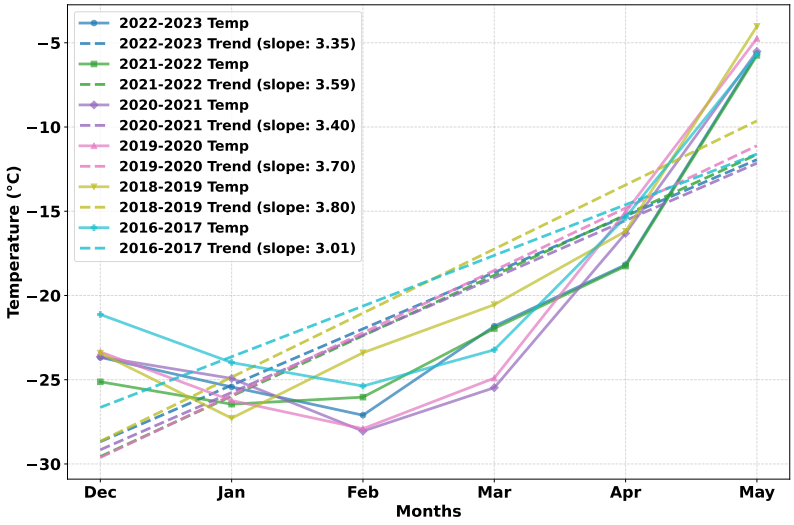


Figure S9. Seasonal Temperature Trends from 2016 to 2023: A comparison of daily temperature variations and trend lines from December to June, highlighting temperature variability across multiple years. The corresponding trend values (slopes) for each season are provided in the legend.

Table S3. Sensitivity of the matched-control analysis of ERA5 10-m wind speed on midpoint-based nominal fracture dates relative to matched non-fracture control days. Controls were selected from the same ice season and calendar month. Here, k is the target number of controls per event; Excl. days is the number of days excluded on either side of fracture dates to avoid overlap with the same synoptic event; N_{matched} is the number of events with valid controls; Coverage is the fraction of the 48 fracture events represented; Med. ctrls is the median number of controls per event; Med. $|\Delta t|$ is the median absolute separation between fracture and control dates; Total is the total number of control days; Med. diff is the median event-minus-control wind-speed difference; and p-val is the two-sided stratified permutation-test probability based on 10,000 permutations. All 48 fracture events were represented in every configuration. The $k = 7$, $\pm$2-day exclusion configuration used for final attribution is shown in bold.

k	Excl. days	N_{matched}	Coverage	Med. ctrls	Med. $\lvert\Delta t\rvert$ (days)	Total	Med. diff (km h^{-1})	p-val
3	1	48	1.00	3	2.0	144	3.736	0.0019
5	1	48	1.00	5	3.0	240	3.254	0.0177
7	1	48	1.00	7	4.0	336	4.737	0.0001
9	1	48	1.00	9	4.0	432	4.376	0.0004
3	2	48	1.00	3	3.0	144	3.536	0.0149
5	2	48	1.00	5	4.0	240	4.719	0.0004
7	**2**	**48**	**1.00**	**7**	**5.0**	**336**	**4.917**	**0.0001**
9	2	48	1.00	9	6.0	432	5.169	0.0002
3	3	48	1.00	3	5.0	144	5.107	0.0005
5	3	48	1.00	5	5.0	240	4.769	0.0002
7	3	48	1.00	7	6.0	336	4.100	0.0016
9	3	48	1.00	9	7.0	428	3.714	0.0153

Oceanographic Controls on Fracture Occurrence

Residual water levels were calculated as the difference between observed and predicted water levels, thereby isolating non-tidal water-level variability associated primarily with meteorological forcing. Daily tidal range, residual water-level metrics, and lunar phase were compared between fracture dates and matched non-fracture control dates. Fractures occurred across a wide range of tidal conditions, with no clear preference for spring tides, neap tides, or particular lunar phases (see Figure S10). Similarly, daily tidal ranges on fracture dates were statistically indistinguishable from those on control dates, indicating that astronomical tidal forcing alone does not control fracture occurrence.

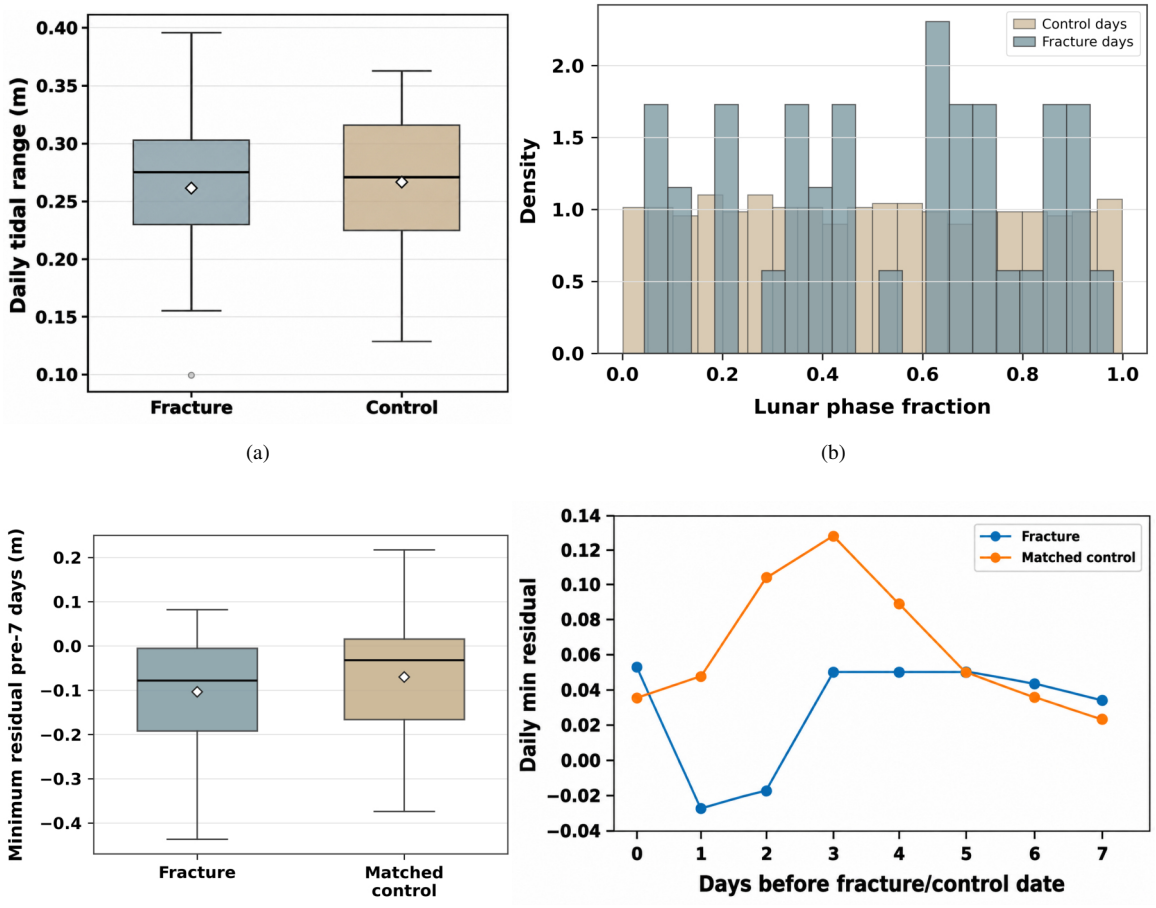


Figure S10. Oceanographic controls on fracture occurrence near Tuktoyaktuk. (a) Comparison of daily tidal range between fracture and matched control dates. (b) Distribution of fracture events relative to lunar phase. (c) Minimum residual water level during the seven days preceding fracture and matched control dates. (d) Lag composite of daily minimum residual water level relative to fracture occurrence.

Residual water levels exhibited a weak tendency toward more negative values on and shortly before fracture occurrence, as shown in Figure S10. These negative residuals correspond to modest coastal drawdown conditions and may slightly reduce hydrostatic support beneath the LFSI, although the signal is weak and temporally variable. However, the observed differences between fracture and control dates were small, showed substantial overlap, and were not statistically significant.

Overall, the oceanographic analyses provide little evidence that tides are a primary driver of fracture formation. While weak negative residual water-level anomalies may contribute to preconditioning the ice cover before some events, the strongest environmental signal identified in this study remains the synoptic-scale atmospheric forcing described in the main manuscript. Atmospheric pressure and pressure-gradient metrics exhibited stronger and more consistent relationships with fracture occurrence than any tide-related variable.